

# Young Supernova Remnants in the Magellanic Clouds

John P. Hughes<sup>1</sup>

<sup>1</sup> *Rutgers University, Department of Physics and Astronomy*

**Abstract.** There are a half-dozen or so young supernova remnants in the Magellanic Clouds that display one or more of the following characteristics: high velocity ( $\gtrsim 1000$  km s<sup>-1</sup>) emission, enhanced metallicity, or a rapidly rotating pulsar. I summarize the current state of knowledge of these remnants and present some recent results mostly from the new X-ray astronomy satellites.

## INTRODUCTION

The Magellanic Clouds (MCs) have been fertile hunting ground for supernova remnants (SNRs) for the last 40 years or so. Early work, focused on the optical [1] and radio [2] bands, resulted in the discovery of the first SNRs in the MCs, N132D, N49, and N63A. Since then deeper radio surveys as well as new X-ray surveys [3] in conjunction with optical spectroscopic follow-up have yielded a grand total of more than 50 confirmed remnants in the Clouds.

The common, well-known distances to the Clouds (50 kpc and 60 kpc for the large and small Clouds, respectively) allow for accurate estimates of such quantities as mass and energy, which have strong dependences on distance ( $D^{5/2}$ ). The Clouds are close enough that angular resolution is not a major limiting factor, particularly now with the superb telescopes on the *Hubble Space Telescope* and *Chandra X-ray Observatory*. The generally low absorption to the Clouds makes possible UV and soft X-ray studies that are often precluded for Galactic remnants and indeed nearly all MC SNRs have been detected in the radio, optical, and X-ray bands. The sample of MC remnants is thus well-defined with reasonably clear selection criteria. With it one can sample the range of remnant types and SN progenitors, as well as probe the dynamical evolution of SNRs.

Since SNRs can exist as distinct entities for tens to hundreds of thousands of years, most of the remnants in the MCs are middle-aged or old. But chronological age alone is not the only determinant of youth; environment plays an equally important role. In a low density environment a remnant will expand to great size and the ejecta can dominate the dynamics and the emission properties for a considerable time. On the other hand, remnant evolution will proceed rapidly in the

densest environments, passing quickly to the radiative phase. Thus a definition of what constitutes a young SNR is needed. Here I will use the following, largely observational, definition. A young remnant is one with a rapidly rotating, high spin-down-rate pulsar; high velocity oxygen-rich optical emission; other evidence for supernova (SN) ejecta; or a kinematic age of roughly 2000 yr or less. Note that I will not discuss SN1987A since it is the subject of an entire article elsewhere in this volume [4].

## A SURVEY OF YOUNG MC REMNANTS

In this section I survey the properties and nature of the known young supernova remnants in the MCs. Objects are introduced in chronological order according to when each was identified as a young SNR, based on the criteria just described.

### N132D

One of the original Large Magellanic Cloud (LMC) SNRs, N132D, can be considered to be young. Originally noted as an optical emission nebula [1] and a continuum radio source [2], N132D was confirmed as a remnant through optical spectroscopy [5]. In 1976 oxygen-rich optical filaments spanning a wide velocity range ( $\sim 4000 \text{ km s}^{-1}$ ) were discovered in the center of N132D [6]. Although this is unquestionably emission from SN ejecta, N132D also shows an outer shell of normal swept-up interstellar medium (ISM) that in fact dominates the integrated X-ray emission [7] and appears to be associated with a giant molecular cloud [8]. N132D was almost surely a core-collapse SN, but no compact remnant has yet been detected. The age of the remnant estimated from the expansion and size of the oxygen-rich filaments is  $\sim 3000$  yrs, while an X-ray spectral analysis yields 2000–6000 yrs [9]. Preliminary results from *Chandra* HETG [10] and *XMM-Newton* [11] observations of N132D are discussed elsewhere in this volume. The EPIC MOS narrowband images of N132D show strong oxygen emission in the center, while at higher energies the most intense emission comes from the southern limb where the remnant is interacting with dense material presumably associated with the molecular cloud that lies there.

### 0540–69.3

It was not until the launch of the *Einstein Observatory* that additional examples of young remnants were discovered in the MCs. Three of the four new young remnants were discovered through their spatially-extended, soft X-ray emission and later identified as optical and radio emission nebulae. (More on them below.) The fourth remnant, SNR 0540–69.3 (also referred to as N158A), was known to be a nonthermal radio source [12] and had been suggested to be a SNR as early as 1973 [13]. High velocity oxygen-rich filaments with velocities spanning  $\sim 3000 \text{ km s}^{-1}$  were discovered [14] soon after the *Einstein* survey of the LMC showed SNR 0540–69.3 to be the third brightest extended soft X-ray source in the Cloud [15]. The X-ray emission is almost entirely nonthermal [16], like the Crab Nebula, and indeed SNR 0540–69.3 also harbors a rapidly spinning compact remnant, in this

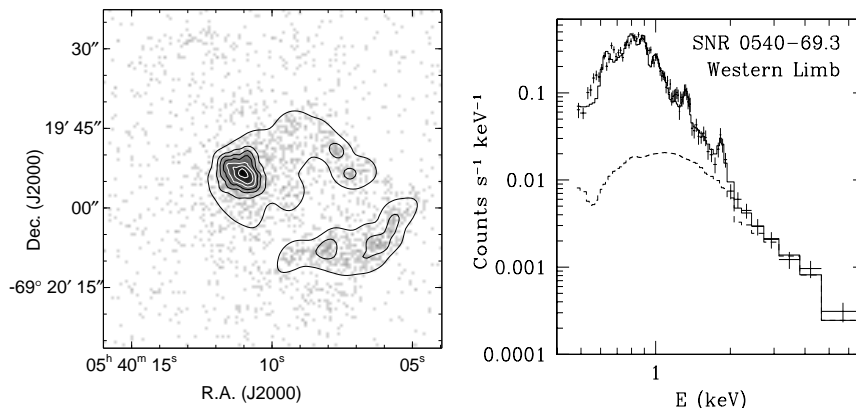


**FIGURE 1.** Left panel shows the HRC image of SNR 0540–69.3 as both raw counts per pixel (grayscale) and adaptively smoothed contours. Right panel shows the ACIS-S CCD spectrum of the faint western limb with thermal model and power law (dashed). Elemental abundances are consistent with swept-up ISM rather than SN ejecta.

case a 50-ms pulsar [17]. The spin-down age of the pulsar  $\tau = P/2\dot{P}$  is roughly 1600 yr, while the kinematic age is  $\sim 800$  yr [18]. This remnant is probably the second youngest SN in the LMC, only exceeded in its youth by SN1987A.

Within the last year *Chandra* HRC observations [19] have revealed the fine-scale structure of the remnant: a patchy incomplete shell surrounding an elliptically-shaped plerionic core that greatly resembles the Crab Nebula (Fig. 1). In the optical band the core, as imaged by *HST*, shows a beautiful filamentary structure with complex spectral variations with position [20]. The ACIS-S CCD spectral data (Fig. 1) show that the shell is swept-up ISM, as opposed to SN ejecta. A nonequilibrium ionization thermal model yields abundances for O, Ne, Mg, Si, and Fe of  $\sim 0.3$  times solar, consistent with the low metallicity of the LMC. Under the plausible assumption that this emission represents the blast wave, then our fitted electron temperature of  $\sim 0.4$  keV is remarkably low for such a young remnant. The X-ray spectrum also requires a hard power law tail with a photon index of  $\alpha \sim 2.5$ . Whether this emission is related to the pulsar itself or is an indication of nonthermal emission at the shock front, like in SN1006 and a few other Galactic remnants, remains to be determined. In any event, as the unique example of an oxygen-rich remnant that also contains a young pulsar, SNR 0540–69.3 is an important object for studying the link between pulsars and the massive stars that form them in core-collapse SNe.

### 1E0102.2–7219

Yet another oxygen-rich remnant was the next young one to be identified in the Clouds. This was also the result of an *Einstein* X-ray survey, this time of the Small Magellanic Cloud (SMC) [21]. The new remnant, 1E0102.2–7219, is the second brightest soft X-ray source in the SMC. Optical follow-up confirmed the identification as a SNR and revealed it to be extremely oxygen-rich [22] with [O

III] emission covering  $\sim 6500 \text{ km s}^{-1}$  in velocity [23]. From this a kinematic age of  $\sim 1000 \text{ yr}$  was estimated. *ASCA* showed the X-ray emission from 1E0102.2–7219 to be dominated by lines from He- and H-like species of O, Ne, Mg, and Si, although it was not possible to obtain a simple interpretation of the integrated spectrum [24]. No compact remnant, either pulsar or plerionic core, has been detected down to a flux limit of  $10^{34} \text{ erg cm}^{-2} \text{ s}^{-1}$  [25]. However, the ACIS-S CCD data did reveal a faint shelf of X-ray emission presumably from the blast wave lying beyond the bright rim of oxygen-rich ejecta [25]. As for the ejecta, *Chandra* HETG line images from the past year reveal high velocity O- and Ne-rich X-ray emitting ejecta with different positions in the shell displaying different red- and blue-shifts [10]. The remnant’s size depends on the emission line under study. In general the remnant appears larger in higher ionization species than it does in lower ones, an effect that is also seen in the lower spectral resolution ACIS-S CCD data [25]. One simple interpretation is that we are seeing the progressive increase in ionization caused by the reverse shock propagating inward through the ejecta. The outermost ejecta material was heated by the reverse shock first and hence has had the most time to ionize up to higher ionization species. The most recently shocked ejecta, however, lies interior to this and should show a lower ionization state. Although qualitatively consistent with the observations, this picture may be oversimplified. In addition to the temporal effect just described, the temperature and density in the ejecta may vary significantly from the contact discontinuity (outside) to the reverse shock (inside) and thereby cause spectral variations with position. The temperature and density variations contain information about the original distribution of matter in the ejecta and the circumstellar medium (CSM) (see, e.g., [26]). Hopefully, further study will allow us to disentangle the effects of time, density, and temperature and learn more about the ejecta and CSM in 1E0102.2–7219.

Very recently my collaborators and I used the *Chandra* ACIS-S CCD data on 1E0102.2–7219 to address some basic issues of shock physics [27]. The question we originally set out to investigate was “To what extent are electrons heated at high Mach number shocks in SNRs?” Do the electrons rapidly attain similar temperatures to the ions through anomalous heating processes driven by plasma instabilities at the shock front (see, for example, [28])? Or do the ion and electron temperatures initially differ by their mass ratio ( $m_p/m_e = 1836$ ) with the electrons subsequently gaining heat slowly from the ions through Coulomb collisions?

Clearly the information needed for this study was the post-shock temperatures of both the electrons and ions. We determined the post-shock electron temperature from fits to the X-ray spectrum of the blast wave region that *Chandra* had revealed for the first time. Fig. 2 shows this spectrum and for comparison the spectrum of a portion of the bright rim of ejecta which displays a markedly different spectral character. The derived abundances from the blast-wave spectrum confirm its origin as swept-up ISM and, for a variety of nonequilibrium ionization spectral models, the derived electron temperature was constrained to be less than 1 keV. It is impossible at the present time to determine the post-shock ion temperature directly (since there is no H line emission from the remnant). We were, however, able to determine

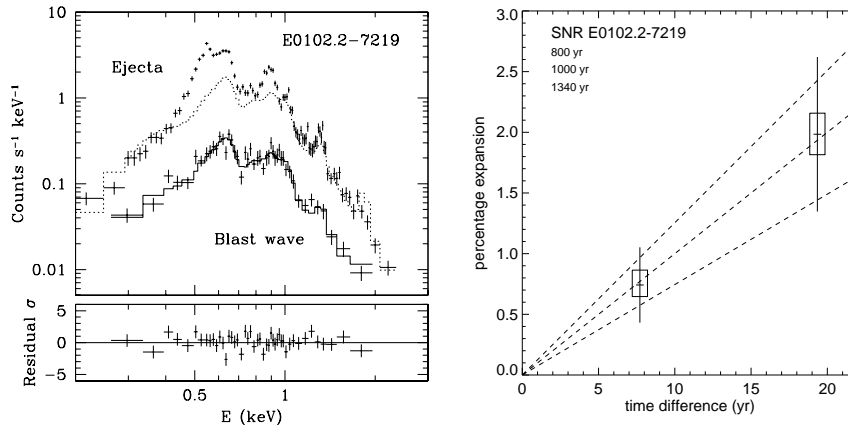


**FIGURE 2.** Left panel shows the ACIS-S CCD spectra of a portion of the outer blast wave and bright rim of ejecta in SNR 1E0102.2–7219. Right panel shows the expansion rate of this remnant from a comparison of the *Chandra* ACIS image with earlier *ROSAT* and *Einstein* images.

the velocity of the blast wave by measuring the angular expansion rate of the remnant. Previous images of 1E0102.2–7219 made by *ROSAT* and *Einstein* were compared to the *Chandra* image and it was found that a significant change in size had occurred (Fig. 2). From the expansion rate ( $0.100\% \pm 0.025\% \text{ yr}^{-1}$ ) and known distance a blast wave velocity of  $\sim 6000 \text{ km s}^{-1}$  was determined. If we assume that the electron and ion temperatures are fully equilibrated at the shock front, then the post-shock electron temperature we measure is about a factor of 25 lower than expected given this blast wave velocity. How low can the post-shock electron temperature be if the post-shock ion temperature is given by the Rankine-Hugoniot jump conditions? This is set by assuming that post-shock electrons and ions exchange energy solely through Coulomb interactions. In this case, we find that the minimum expected electron temperature is  $\sim 2.5 \text{ keV}$ , still significantly higher than what we measure. Our explanation for this discrepancy is that efficient shock acceleration of cosmic rays has reduced the post-shock temperature of both the electrons and ions [29], or in other words, a large fraction of the shock energy has been diverted from the thermal particles and has instead gone into generating relativistic particles, which produce the remnant’s radio emission [30]. Nonlinear models for efficient shock acceleration of cosmic rays [31] predict mean post-shock electron and ion temperatures of 1 keV for high Mach number shocks, i.e., 100–300, as appropriate to 1E0102.2–7219, lending strong quantitative support for this scenario.

#### E0509–67.5 and E0519–69.0

E0509–67.5 and E0519–69.0 are two apparently similar SNRs in the LMC that were discovered through their X-ray emission [3]. Their X-ray morphologies are strongly shell-like and reasonably symmetric. Optical follow-up [32] revealed them to be members of a rare class of faint SNRs, like Tycho and SN1006 in the Galaxy,

that are dominated by Balmer line emission and show little or no forbidden line emission from, e.g., [O III] or [S II]. Like their Galactic cousins, these two LMC SNRs were originally believed to be young in part because they are among the smallest remnants in the LMC with diameters of 7 pc (E0509–67.5) and 8 pc (E0519–69.0). In addition for E0519–69.0, at least, there is evidence for a broad component to H $\alpha$  with FWHM velocity widths ranging from 1300 km s<sup>-1</sup> [33] to 2800 km s<sup>-1</sup> [32]. This emission arises from charge exchange between fast protons and neutral hydrogen atoms in the immediate post-shock region [34] with the width of the line being related to the shock velocity and assumptions about the post-shock partition of energy into hot electron, ions, and cosmic rays [35]. The broad line in E0519–69.0 implies a probable shock velocity range of 1000–1900 km s<sup>-1</sup> (although there are likely to be significant variations with position) and an age of 500–1500 yrs [33]. No broad H $\alpha$  has yet been detected from E0509–67.5 which has been interpreted as implying a lower limit on the actual shock velocity in the remnant of >2000 km s<sup>-1</sup> with a corresponding upper limit on the age of <1000 yr [33]. *ASCA* observations of these remnants [36] revealed the spectacular ejecta-dominated nature of their integrated X-ray emission. The spectra are dominated by a broad quasi-continuum emission of unresolved Fe L-shell lines around 0.7–0.9 keV as well as strong K $\alpha$  lines of highly ionized Si, S, Ar, and Ca. The spectra were shown to be qualitatively consistent with the nucleosynthetic products expected from a Type Ia SN explosion, thereby significantly strengthening the connection between Balmer-dominated SNRs and the remnants of Type Ia SN.

Early *Chandra* results on E0519–69.0 [37] show an integrated spectrum quite similar to the *ASCA* one, but the lower effective background of the *Chandra* data allows for clear detection of the important Fe K $\alpha$  line. There are spatial/spectral variations across the remnant with the most notable difference being a strong increase in emission in the 0.5–0.7 keV band at the rim.

The *Chandra* broad-band X-ray image of E0509–67.5 is shown in Fig. 3 along with the integrated spectrum. The shell is quite round, nearly complete, and brightest on the western side; all of which are quite similar to the H $\alpha$  morphology [33]. The intensity fluctuations around the bright limb of the remnant are generally significant with peak to valley brightness variations of about a factor of two on spatial scales of just a few arcseconds. Whether this apparent clumping of the ejecta originated during the SN explosion process itself, arose later on through Rayleigh-Taylor instabilities from interaction with the ambient medium, or has some other origin remains to be investigated. There is no morphological evidence for a double shock structure: the X-ray emission is dominated by metal-rich ejecta and no outer blast wave component is detected. Again the spectrum is quite similar to the *ASCA* one [36], although here with *Chandra* we have detected Ar, Ca, and Fe K $\alpha$  line emission at energies of 3.0 keV, 3.7 keV, and 6.4 keV, respectively. The Si and S K $\alpha$  lines in the integrated spectrum of E0509–67.5 are quite strong (equivalent widths of 1.9 keV for Si and 1.2 keV for S), very broad (FWHM line widths of 100 eV and 120 eV), and appear at much lower energies than the He- and H-like K $\alpha$  lines should (mean line energies are 1.804 keV and 2.377 keV). There is

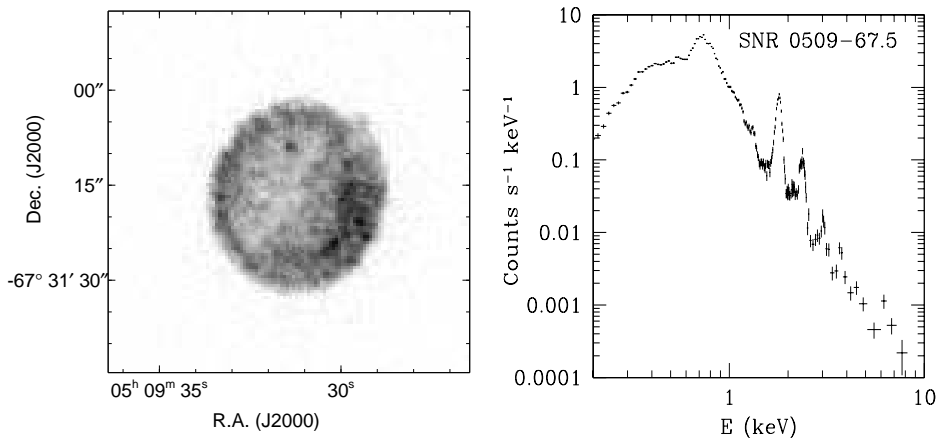


**FIGURE 3.** Left panel shows the ACIS-S CCD image of E0509–67.5 over the 0.2–7.0 keV band. Right panel shows the integrated spectrum of the remnant.

no change in the width or mean energy of the Si  $K\alpha$  line with radius, which argues against velocity effects (which would have to be enormous anyway) as the source of the line broadening. The most likely explanation for the broad Si line is that it is a blend of lines from a wide range of charge states, i.e., from  $\text{Si}^{12+}$  (He-like) to  $\text{Si}^{5+}$  or lower. A similarly broad range of charge states for S is required to explain that broad line. It seems likely that a range of temperatures or ionization timescales will be necessary to account for the broad lines; simple planar shock models tend to produce too narrow a distribution of charge states. The spectral analysis with radius does reveal one significant variation—the Si line equivalent width drops by a factor of 2 (to a value of  $\sim 1$  keV) right at the edge of the remnant—perhaps an indication of some dilution of the ejecta emission by a component of swept-up ISM.

### N103B

First identified in 1973 as a SNR based on its radio and optical properties [13], N103B was detected as an extended, soft X-ray source by the *Einstein Observatory* [15]. It is the fourth brightest X-ray remnant in the LMC and is also one of the smallest LMC SNRs ( $\sim 7$  pc in diameter). Optically the remnant consists of several small, bright knots visible in  $\text{H}\alpha$ ,  $[\text{O III}]$ , and  $[\text{S II}]$ . Its proximity to the star cluster NGC 1850 and the H II region DEM 84 led to the suggestion that SNR N103B had a population I progenitor [38]. It was not until *ASCA* that N103B was revealed to be young based on its ejecta-dominated spectrum [36]. The surprising result was that the X-ray spectrum of N103B bears a remarkable similarity to the Balmer-dominated SNR E0519–69.0 and indeed both remnants are now believed to be remnants of Type Ia SN. The *Chandra* data [39] show a highly structured remnant that is much brighter on the western limb than toward the east. On large scales it resembles the radio remnant [40] but on finer spatial scales the bright radio and X-ray emission features tend not to overlap. There are complex spatial/spectral variations across the remnant including changes in the equivalent width of the He-

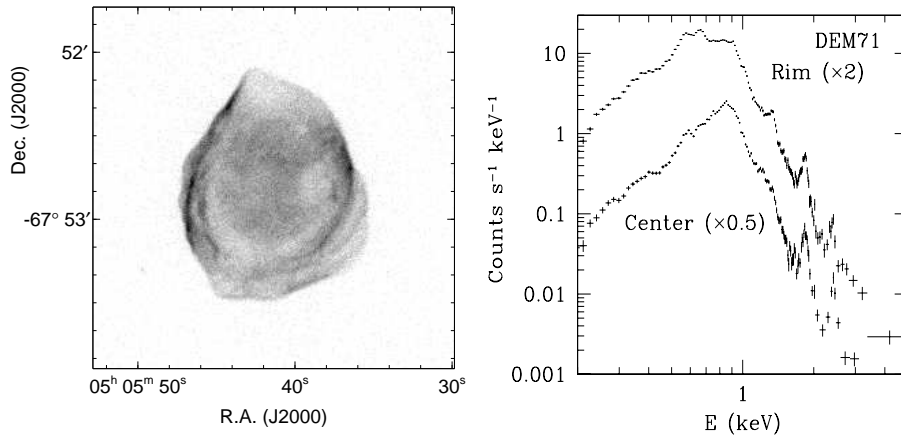


**FIGURE 4.** Left panel shows the ACIS-S CCD image of DEM71 over the 0.2–4.4 keV band. Right panel shows the spectrum of the remnant from the outer rim and the central region.

like Si  $K\alpha$  emission line which appears to increase radially outward. In contrast to E0509–67.5, the Si  $K\alpha$  line from N103B shows both a He- and H-like component indicating that N103B is at a higher mean ionization state.

#### N157B

Originally detected as a nonthermal radio source [12], and suggested as a possible SNR in 1973 [13], it was not until extended soft X-rays were detected by the *Einstein Observatory* [15] that N157B (also referred to as 30 Dor B) was confidently confirmed as a remnant. Its featureless powerlaw X-ray spectrum [16] and flat radio spectral index ( $\alpha \sim -0.19$  [41] [42]) were taken as strong evidence that the remnant was Crab-like and should contain a rapidly rotating pulsar. The pulsar in N157B was discovered in 1998 [43] with a spin period of 16.1 ms making it the fastest known pulsar in a SNR. The spin-down rate of  $\dot{P} = 5.126 \times 10^{-14} \text{ s s}^{-1}$  implies a characteristic age of  $\tau = 5000 \text{ yr}$  which agrees well with other estimates of the remnant’s age [44].

#### DEM71

A new example of a possible young SNR is DEM71. Initially noted as an optical nebula [45], it was detected as an extended soft X-ray source by *Einstein* and proposed as a SNR [3]. Optical follow-up revealed it to be a Balmer-dominated remnant [32] with broad  $H\alpha$  line emission [33]. Given its size (20 pc diameter) and shock velocity of  $\sim 500 \text{ km s}^{-1}$  (estimated from the broad  $H\alpha$  line), the remnant is  $\sim 8000 \text{ yr}$  old. *ASCA* spectroscopy revealed the first tantalizing hints of youth for this SNR in the form of an enhanced abundance of Fe [9].

The broadband image of DEM71 from *Chandra* (fig. 4) shows emission from an outer rim that matches nearly perfectly the optical  $H\alpha$  image, including the brightness of the eastern and western rims as well as the multiple filaments along the southern edge. The nearly circular, faint, diffuse emission that almost fills the interior has no counterpart in the optical band [41]. The ACIS-S CCD spectrum



of the center (Fig. 4) is dominated by a broad quasi-continuum of emission near 1 keV from Fe L-shell lines, plus Si and S  $K\alpha$  lines at higher energy. This spectrum is grossly different from that of the outer rim, which is generally softer and shows prominent O and Mg  $K\alpha$  lines. We propose that the rim represents the blast wave moving out into the ambient interstellar medium, while the interior emission is the reverse shock propagating through iron-rich ejecta. Detailed study of the *Chandra* data is now underway using the outer rim emission to study the basic physics of SN shocks and the central Fe-rich emission to investigate the evolution of metal-rich ejecta in SNRs.

## CONCLUSIONS

I expect the list of “young” remnants in the MCs to grow as improvements in sensitivity make it easier to identify youthful aspects of older known remnants. It is likely that there are still a few pulsars left to be discovered in the MC SNRs either through direct measurement of pulsed radiation or from the identification of their associated pulsar-wind nebulae. If DEM71 can be considered to be a guide, then even remnants that are several thousand years old can show evidence for SN ejecta. N63A, N49, N23 in the LMC, all of which are smaller in size than N132D and DEM71, are in this age range and therefore have the potential for showing traits of youth. It will be worth keeping an eye on these remnants in the coming years.

*Acknowledgments* I gratefully acknowledge Dave Burrows, Anne Decourchelle, Gordon Garmire, Parviz Ghavamian, Karen Lewis, John Nousek, Cara Rakowski, and Pat Slane for their collaborations on various studies of MC SNRs. I would also like to thank Andy Rasmussen and Ehud Behar for sharing XMM results prior to publication. This work was partially supported by *Chandra* General Observer grant GO0-1035X.

## REFERENCES

1. Henize, K.G. 1956, ApJS, 2, 315.
2. Mathewson, D.S., & Healey, J.R. 1964, The Galaxy and the Magellanic Clouds, ed., F. R. Kerr & A. W. Rodgers (Canberra: Australian Academy of Science) p. 283.
3. Long, K.S., Helfand, D.J., & Grabelsky, D.A. 1981, ApJ, 248, 925.
4. McCray, R., et al. 2001, this volume.
5. Westerlund, B. E., & Mathewson, D.S. 1966, MNRAS, 131, 371.
6. Danziger, I.J., & Dennefeld, M. 1976, ApJ, 207, 394.
7. Hughes, J.P. 1987, ApJ, 314, 103.
8. Banas, K.R., Hughes, J.P., Bronfman, L., & Nyman, L.-Å. 1997, ApJ, 480, 607.
9. Hughes, J.P., Hayashi, I., & Koyama, K. 1998, ApJ, 505, 732.
10. Canizares, C., et al. 2001, this volume.
11. Behar, E., et al. 2001, this volume.

12. Le Marne, A.E. 1968, MNRAS, 139, 461.
13. Mathewson, D.S., & Clarke, J.N. 1973, ApJ, 180, 725.
14. Mathewson, D.S., Dopita, M.A., Tuohy, I.R., & Ford, V.L. 1980, ApJ, 242, L73.
15. Long, K.S., & Helfand, D.J. 1979, ApJ, 234, L77.
16. Clark, D.H., Tuohy, I.R., Long, K.S., Szymkowiak, A.E., Dopita, M.A., Mathewson, D.S., & Culhane, J.L. 1982, ApJ, 255, 440.
17. Seward, F.D., Harnden, F.R., & Helfand, D.J. 1984, ApJ, 287, L19.
18. Kirshner, R.P., Morse, J.A., Winkler, P.F., & Blair, W.P. 1989, ApJ, 342, 260.
19. Gotthelf, E.V., & Wang, Q.D. 2000, ApJ, 532, L117.
20. Morse, J.A., et al. 2001, in prep. (shown at the conference by W.P. Blair).
21. Seward, F.D., & Mitchell, M. 1981, ApJ, 243, 736
22. Dopita, M.A., Tuohy, I.R., & Mathewson, D.S. 1981, ApJ, 248, L105.
23. Tuohy, I.R., & Dopita, M.A. 1983, ApJ, 268, L11.
24. Hayashi, I., Koyama, K., Ozaki, M., Miyata, E., Tsunemi, H., Hughes, J.P., & Petre, R. 1994, PASJ, 46, L121.
25. Gaetz, T.J., Butt, Y.M., Edgar, R.J., Eriksen, K.A., Plucinsky, P.P., Schlegel, E.M., & Smith, R.K. 2000, ApJ, 534, L47.
26. Chevalier, R.A. 1982, ApJ, 258, 790.
27. Hughes, J.P., Rakowski, C.E., & Decourchelle, A. 2000, ApJ, 543, L61.
28. Cargill, P.J., & Papadopoulos, K. 1988, ApJ, 329, L29.
29. Blanford, R.D., & Eichler, D. 1987, Phys. Rep., 154, 1.
30. Amy, S.W., & Ball, L. 1993, ApJ, 411, 812.
31. Ellison, D.C. 2000, in AIP Conf. Proc. 529, Acceleration and Transport of Energetic Particles Observed in the Heliosphere, ed. R.A. Mewaldt, et al. (New York AIP), 386.
32. Tuohy, I.R., Dopita, M.A., Mathewson, D.S., Long, K.S., & Helfand, D.J. 1982, ApJ, 261, 473.
33. Smith, R.C., Kirshner, R.P., Blair, W.P., & Winkler, P.F. 1991, 375, 652.
34. Chevalier, R.A., & Raymond, J.C. 1978, ApJ, 225, L27.
35. Chevalier, R.A., Kirshner, R.P., & Raymond, J.C. 1980, ApJ, 235, 186.
36. Hughes, J.P., et al. 1995, ApJ, 444, L81.
37. Williams, R.M., et al. 2001, this volume.
38. Chu, Y.-H., & Kennicutt, R.C. 1988, AJ, 96, 1874.
39. Lewis, K.T., Burrows, D.N., Nousek, J.A., Garmire, G.P., Slane, P., & Hughes, J.P. 2001, this volume.
40. Dickel, J., & Milne, D. 1995, AJ, 109,1.
41. Mathewson, D.S., Ford, V.L., Dopita, M.A., Tuohy, I.R., Long, K.S., & Helfand, D.J. 1983, ApJS, 51, 345.
42. Lazendic, J.S., Dickel, J.R., Haynes, R.F., Jones, P.A., & White, G.L. 2000, ApJ, 540, 808.
43. Marshall, F.E., Gotthelf, E.V., Zhang, W., Middleditch, J., & Wang, Q.D. 1998, ApJ, 499, L179.
44. Wang, Q.D., & Gotthelf, E.V. 1998, ApJ, 494, 623.
45. Davies, R.D., Elliott, K.H., & Meaburn, J. 1976, Mem. R.A.S., 81, 89.